

## Properties and nature of Be stars<sup>★,★★</sup>

### 25. A new orbital solution and the nature of a peculiar emission-line binary $\nu$ Sagittarii

P. Koubský<sup>1</sup>, P. Harmanec<sup>2,1</sup>, S. Yang<sup>3</sup>, M. Netolický<sup>4,1</sup>, P. Škoda<sup>1</sup>, M. Šlechta<sup>1</sup>, and D. Korčáková<sup>1</sup>

<sup>1</sup> Astronomical Institute, Academy of Sciences, 251 65 Ondřejov, Czech Republic  
e-mail: koubsky@sunstel.asu.cas.cz

<sup>2</sup> Astronomical Institute of the Charles University, V Holešovičkách 2, 180 00 Praha 8, Czech Republic

<sup>3</sup> Department of Physics and Astronomy, University of Victoria, PO Box 3055 STN CSC, Victoria, B.C. V8W 3P6, Canada

<sup>4</sup> Institute of Theoretical Physics and Astrophysics, Faculty of Science, Masaryk University Brno, Kotlářská 2, 602 00 Brno, Czech Republic

Received 25 March 2006 / Accepted 28 April 2006

#### ABSTRACT

**Context.** Binaries observed in the initial rapid phase of mass exchange between the components are very rare since the statistical probability of finding them is low. At the same time, thorough studies of them are extremely important for better understanding the process of large-scale mass exchange and possible mass loss from the system. One of these objects is probably  $\nu$  Sgr.

**Aims.** By analyzing 35 new electronic spectra and numerous published spectral and photometric observations, we derived the new orbital elements, an upper limit to a secular period change, and also the peculiar RV curve of the blue-shifted  $H\alpha$  absorption. Possible models of the binary and its evolutionary stage are then discussed critically.

**Methods.** Reduction of new spectra was carried out with the IRAF and SPEFO programs. All orbital elements were derived with the FOTEL program and period searches were carried out using the phase-dispersion minimalization technique.

**Results.** The peculiar RV curve of the blue-shifted  $H\alpha$  absorption rules out the model of a coronal flow of matter from the brighter component. The presence of bipolar jets that are perpendicular to the orbital plane and similar to those found for  $\beta$  Lyr seems probable. An upper limit to the secular period decrease of 24 s per year was estimated and should be tested by future RV observations. The peculiar character of the line spectrum of the brighter component could also be understood as originating from a pseudo-photosphere of an optically thick disk rather than from a stellar spectrum.

**Conclusions.** Better understanding of the nature of  $\nu$  Sgr will not be possible without interferometric resolution of the binary and especially without determining its orbital inclination.

**Key words.** stars: emission-line, Be – stars: binaries: close – stars: individual:  $\nu$  Sagittarii

#### 1. Current knowledge about $\nu$ Sgr

The emission-line binary  $\nu$  Sgr (46 Sgr, HD 181615, HR 7342, HIP 95176, MWC 313;  $V = 4^m.6$  var.) is a very unusual object. Its radial-velocity (RV hereafter) variations were discovered by Campbell (1899). Wilson (1913) later demonstrated that  $\nu$  Sgr is a single-line spectroscopic binary and derived its first orbital elements:  $P = 137^d.939$ ,  $e = 0.087$ ,  $\omega = 28^{\circ}.6$ , and  $K = 48.15 \text{ km s}^{-1}$ . Duvignau et al. (1979) studied OAO3 and TD1 satellite UV spectra and concluded that the far-UV spectra resemble a B0Ia object. From the absence of measurable RV variations of high-excitation lines, they deduced that the companion must be much more massive than the object seen in the optical spectra. Parthasarathy et al. (1986) came to similar conclusions on the basis of the IUE spectra.

\* Based on the spectroscopic observations secured with the telescopes and spectrographs of the Dominion Astrophysical Observatory and Ondřejov Observatory.

\*\* Table 2 is only available in electronic form at the CDS via anonymous ftp to cdsarc.u-strasbg.fr (130.79.128.5) or via <http://cdsweb.u-strasbg.fr/cgi-bin/qcat?J/A+A/459/849>

The only real RV measurements of the fainter component by Dudley & Jeffery (1990) are based on the cross-correlation of the far-UV spectra from the short-wavelength camera on board the IUE satellite. These authors also derived RVs of the component observed in the optical region, using all high-dispersion SWP and LWP IUE spectra with a good S/N ratio. They concluded that the eccentricity of the orbit is spurious and went on to derive a circular orbit. Analyzing all the available RVs, they also concluded that there were no detectable changes in the orbital period. Perhaps the most important result of their study is the finding that the mass ratio of the “invisible” to visible binary component is 1.59, i.e. that the invisible star is the more massive of the two. Dudley & Jeffery (1990) also concluded that the luminosity ratio of the visible to “invisible” component must be about 100. However, in a later paper Dudley & Jeffery (1993) show that such an extreme luminosity ratio is inconsistent with the observed high flux shortwards of 1400 Å and that the source of this excess is in the vicinity of the “invisible” star. Furthermore, the deconvolved spectrum of that component presented in Dudley & Jeffery (1990) is characterized by a number of features of either interstellar or circumstellar origin.

The “invisible” component might be imbedded in an envelope, which also makes the RV determination and thus the value of the system mass ratio uncertain. The detection of the secondary RV curve therefore deserves an independent verification. At the present stage of knowledge,  $\nu$  Sgr seems to bear some similarity to  $\beta$  Lyr, because the component that would normally be called *primary* on the basis of its relative brightness could also be called *secondary* on the basis of its mass. To avoid confusion, we call the star dominating the optical and UV line spectra *star 1* in the rest of this paper and its (probably more massive but less luminous) counterpart *star 2*.

A strong  $H\alpha$  emission in the spectrum of  $\nu$  Sgr was reported by Campbell (1895) and by many other investigators. Maury (1925) called attention to another peculiarity of the object: the optical spectrum contains lines that resemble an F2 supergiant but also a B8 spectrum, and the relative strength of these two spectra varies in time, the B8 spectrum being strongest at phases of a conjunction in which star 2 is in front of star 1. Such a variation in the relative strength of the hot and cool spectra was not observed in later studies (based on better spectra) by Greenstein & Adams (1947) and Greenstein (1950).

Even more puzzling is that the RVs of spectral lines corresponding to “F2” and “B8” spectra follow the same RV curve and are, therefore, associated with star 1 (Plaskett 1926). Maury (1925) also reports that another system of absorption lines was sometimes observed on the Harvard spectrograms, indicating RVs of about  $-280 \text{ km s}^{-1}$ . She pointed out that this system of lines could hardly represent the orbital motion of star 2 since no similarly high positive RVs had ever been observed. Bidelman (1949) investigated these blue-shifted lines further, concluded that they only occur around the phases of the conjunction with star 2 in front of star 1 (but not every orbital cycle), and was probably the first to suggest that they may indicate a gas stream from star 1 towards star 2. Hack (1960) also analyzed high-dispersion  $H\alpha$  line profiles and concluded that the blue-shifted absorption is indeed strongest near the superior conjunction of star 1 but present with progressively reduced strength throughout the whole orbital cycle. Not considering her finding, Nariai (1967) collected and analyzed available  $H\alpha$  profiles, including new ones he obtained at Okayama, and interpreted the blue-shifted lines as a supersonic flow from the stellar corona of star 1 to a cone in the vicinity of star 2. Frame et al. (1995) studied echelle spectra secured in the years 1988, 1991, and 1992. They observed the blue-shifted  $H\alpha$  absorption only on a single 1991 spectrum, although they observed the star near the superior conjunction on seven other dates in 1988 and 1992. Instead, they detected strong  $H\alpha$  emission with a flat red wing, extending to some  $+500 \text{ km s}^{-1}$ .

There is ample evidence that the continuum energy distribution of  $\nu$  Sgr is also composite and is a peculiar one from the IR to UV (Treffers et al. 1976; Hack 1980; Burnashev 1981; Plavec 1986; Jaschek et al. 1990). Gaposchkin (1945) obtained photographic photometry and concluded that  $\nu$  Sgr is an eclipsing binary with two low-amplitude minima, the eclipse of star 2 being deeper than the opposite one. Eggen et al. (1950) published the first photoelectric yellow and blue photometry from Lick. They also obtained a double-wave light curve with 0<sup>m</sup>.1 deep minima. However, they pointed out that the minima occur some 12 days later than predicted from the RV curve and noted that Gaposchkin’s minima also occur some 7 days after the spectroscopic prediction. Burnashev (1981), Malcolm & Bell (1986), and Frame et al. (1995) also obtained photoelectric light curves and found variations on a time scale of about 20 days but no clear evidence of binary eclipses.

Hack & Pasinetti (1963) demonstrated that the chemical composition of star 1 is a peculiar one. They found a strong deficiency of hydrogen and overabundance of C, N, and some other ions. They interpreted it as a consequence of a large-scale mass transfer between the binary components, as did Plavec (1986). Dudley & Jeffery (1993) used published photometry, spectrophotometry and line-blanketed hydrogen-deficient model atmospheres to estimate the effective temperature of star 1 as  $11\,800 \pm 500 \text{ K}$ . Leushin (2001) derived the effective temperature of  $13\,500 \pm 150 \text{ K}$ ,  $\log g = 2 \pm 0.5$ , and the iron abundance for star 1 and reviewed the previous studies of  $\nu$  Sgr done with his collaborators.

Schoenberner & Drilling (1983) have presented an evolutionary scenario for  $\nu$  Sgr. They suggest that star 1 is filling its Roche lobe and spilling its now helium-rich envelope towards star 2 (i.e. that it undergoes the so called case BB of mass exchange). Eggleton (2002) suggests that the binary had to lose mass via envelope ejection, without removal of too much orbital momentum so that a long orbital period and not too extreme mass ratio of 0.63 were preserved.

## 2. Observations and data reduction

Our observations consist of two series of red CCD spectra secured at the Dominion Astrophysical Observatory (DAO hereafter) and in Ondřejov. The initial reductions to 1D frames were carried out in IRAF; by SY for the DAO and by MŠ for the Ondřejov spectra. The final reduction, rectification, RV and line-intensity measurements were carried out in SFEFO (Horn et al. 1996; Škoda 1996) by PK and partly also by PH. The RV’s were measured interactively, comparing the direct and reverse images of the line profiles. The zero point of the RV scale was corrected through the use of reliable telluric lines. For the orbital RV we finally used the mean of the strong, well-defined, and unblended lines, which give consistent results: Ne I 6402.2455 Å and C II 6578.052 Å<sup>1</sup>.

We also compiled all RVs available in the astronomical literature. In all cases when the heliocentric Julian dates (HJDs hereafter) were not tabulated in the original source, we used a computer program to derive HJDs for the data set in question. A few remarks on some of the data sources are in order.

*File 5: IUE RVs* Dudley & Jeffery (1990) tabulate Julian dates only as integers. We extracted HJDs for the mid-exposures for all their RVs and noted one misprint in their paper: JD of the spectrum LWR2276 is 2443 757 (HJD 2443 756.7729), not 2443 557 as given in Table 1 of Dudley & Jeffery (1990). Note that these authors also tabulate 11 RVs of the secondary derived via a cross-correlation technique from some of the SWP spectra.

*File 7: Mt. John echelle spectrograph* Frame et al. (1995) tabulate 33 RVs in their Table 5, but a phase plot of these RVs gives a phase diagram that differs slightly from the phase plot in their Fig. 6. In particular, Fig. 6 does not show an RV value of  $-48 \text{ km s}^{-1}$  observed on JD 2448 377.40 although the numbers of RVs listed in Table 5 and plotted in Fig. 6 are the same. At our inquiry, Dr. Peter Cotrell kindly informed us that the peculiar RV value, corresponding to an anomalous  $H\alpha$  profile, was

<sup>1</sup> The measured RV of the other member of the C II doublet turned out to be influenced by a nearby weak emission line and a telluric line at certain orbital phases – see Fig. 3. The same figure shows that, although the spectral lines vary slightly in their strengths and widths, no clear phase dependence could be established.

**Table 1.** Journal of RV data: the telescopes and spectrographs with which the RVs were obtained, denoted by the running numbers in column “Spg. No.”, are as follows: 1... James Lick 0.91-m refractor, Mills 3-prism spg, phot. plates; 2... Yerkes 1.02-m refractor, Bruce 1-prism spg. phot. plates; 3... DAO Plaskett 1.8-m reflector, Cass. IM or IS prism spgs., phot. plates; 4... Mt. Wilson Hooker 2.54-m reflector, coudé grating spg., 114-inch camera, phot. plates; 14... Mt Wilson Hooker 2.54-m reflector, coudé grating spg., 32-inch camera, phot. plates; 5... IUE satellite 0.45-m reflector, Cass. echelle spgs., SWP, LWP and LWR SEC Vidicon cameras; 6... CTIO 1-m reflector, Cass. spg., image tube & phot. plates; 7... MJUO McLellan 1-m reflector, Cass. fiber fed echelle spg., Reticon 1872; 8... SAAO 1.9-m reflector, Cass spg., image tube & intensified Reticon; 9... DAO McKellar 1.2-m reflector, coudé spg., SITE-4 4096  $\times$  2048 CCD; 10... Ondřejov 2-m reflector, coudé spg., SITE-005 800  $\times$  2000 CCD.

Spg. No.	Time interval (HJD-2 400 000)	No. of lines measured	No. of RVs	Dispersion ( $\text{\AA mm}^{-1}$ )	Resolution	Weight	Source
1	13 742.8–20 256.0	15–25	36			1.025	Wilson (1913)
2	17 843.6–19 295.6	tens	24	30	5000	0.716	Frost et al. (1926)
3	24 127.5–24 714.8	$\geq 30$	24	29&49	5000	0.688	Plaskett (1926)
4	29 500–31 715	tens to hundred	7	2.8	10000	0.940	Greenstein & Adams (1947) <sup>a</sup>
14	30 926–31 004	hundreds	3	20	5000	0.701	Greenstein & Merrill (1946) <sup>a</sup>
4	31 990–34 975	hundreds	10	2.8	10000	0.940	Hack & Pasinetti (1963) <sup>a</sup>
5	43 620.7–46 345.1	cross-correlation	31	$\sim 1$	12000	1.164	Dudley & Jeffery (1990)
6	44 422.7–44 810.8	cross-correlation	6	43	3000	0.837	Jeffery et al. (1987)
7	47 273.7–48 950.4	tens(?) near H $\alpha$	33	2.0	45000	1.863	Frame et al. (1995) <sup>b</sup>
8	47 312.5–47 314.5	cross-correlation	2	30?	5000	1.043	Dudley & Jeffery (1990)
9	53 587.8–53 651.6	2	14	10.1	18000	0.765	this paper
10	53 594.4–53 674.2	2	21	17.2	10000	1.380	this paper

<sup>a</sup> Inaccurate Julian days, tabulated only as integers. <sup>b</sup> Less accurate Julian days, tabulated only to two decimal digits.

not used in their study. He also communicated another observation missing from Table 5 but plotted in Fig. 6: JD 2 447 464.50 with  $RV = +9 \text{ km s}^{-1}$ .

The journal of all RVs used in this study is in Table 1 and all individual RVs with HJDs and weights are tabulated in Table 2 (available only in electronic form).

### 3. A new orbital solution and improved ephemeris

All orbital solutions presented in this study were derived with the computer program FOTEL (Hadrava 2004). To derive new orbital elements, we proceed as follows.

We initially used only the RVs of star 1 and assumed a circular orbit. First we derived a solution in which weights of all RVs were set equal to one. This is solution 1 in Table 3. Then, we made the weights of individual data sets inversely proportional to the square of their rms errors per 1 observation, which were derived in the preliminary solution with equal weights and normalized in such a way that the mean rms per 1 observation from this solution derived for all data was set equal to one<sup>2</sup>. All other exploratory solutions, as well as the final solution, were derived with these weights (which are also given in Table 1).

Solution 2 is a circular-orbit solution for all RVs of star 1 with the weights assigned to all individual data sets. This is the solution that we adopt as the solution defining the following linear ephemeris (1) to be used in this study:

$$T_{\text{max,RV}} = \text{HJD } 2\,433\,018.13 + 137^{\text{d}}9343 \cdot E. \quad (1)$$

By deriving several trial solutions for various, more numerous data subsets, we found that virtually all give a better fit for a slightly eccentric orbit with  $e \sim 0.05$  and  $\omega \sim 0^\circ$ . This is reminiscent of a typical distortion of the curves of emission-line binaries – see, e.g. Fig. 3 in Harmanec (1985) or the detailed discussion in Hill et al. (1997) and Koubský et al. (1997) – and we

<sup>2</sup> Dataset 8 consists of only 2 RVs obtained at very similar orbital phases. This leads to a very small rms error for this dataset and the weighting scheme we use would strongly overestimate the weight of this dataset. We therefore kept the weight of dataset 8 equal to 1.

are inclined to believe that the eccentricity is spurious. However, since the reality of an eccentric orbit with a similar value of  $\omega$  cannot be fully excluded without further, independent pieces of evidence, we also tabulated the eccentric-orbit solution 3 in Table 3.

In yet another solution 4, we fixed the value of the orbital period from ephemeris (1) and derived a *circular* solution for all star-1 RVs and for all RVs of star 2 obtained by Dudley & Jeffery (1990). Note that we tabulated the systemic velocity and the rms errors per 1 observation of unit weight separately for the primary and secondary RVs for this solution.

We also addressed the question of the secular constancy of the orbital period again. Using the RVs of star 1, we derived two circular-orbit solutions for older and more recent data. The main results are in Table 4.

This result is inconclusive. It indicates a 1- $\sigma$  possibility that the orbital period is secularly *decreasing*. We derived a solution for all primary RVs allowing the period change as one of the elements. We obtained a period change

$$dP/dt = (-7.6 \pm 5.3) \times 10^{-5} \text{ d per day i.e. } -24 \text{ s per year,}$$

again a 1- $\sigma$  result. We only use this finding as an estimate of an upper limit of the period change. Its verification with new observations would be very important, however. If  $\nu$  Sgr is currently in a phase of mass exchange, a decreasing orbital period would identify it as an object in the *rare initial rapid phase of mass exchange* before the role of components was interchanged<sup>3</sup>.

A more detailed inspection of Fig. 1 and Table 3 shows that the scatter of RVs around the mean orbital curve is higher than expected for easily measurable sharp lines of star 1. A part of the effect could be caused by the fact (mentioned earlier) that different lines seem to give slightly different RVs for the same spectrograms. To investigate the reality of effect, we therefore plot the new DAO and Ondřejov RVs vs. time in Fig. 2. One can see that there is little doubt about the reality of small cyclic

<sup>3</sup> It is known that during the process of mass exchange, the conservation of the orbital angular momentum causes a decrease in the orbital period until the masses of binary components get interchanged.

**Table 3.** Various orbital solutions for  $\nu$  Sgr derived with the FOTEL program. All epochs are in HJD-2 400 000 and the rms error is error per 1 observation of unit weight. Systemic velocities of individual spectrographs are identified by the running numbers corresponding to those from Table 1. Rather large differences in the individual systemic velocities probably do not reflect real changes but rather compensate for the differences in line identifications and various subsets of lines used by various authors to derive the published RVs.

Element	Solution 1	Solution 2	Solution 3	Solution 4
$P$ (d)	$137.9331 \pm 0.0022$	$137.9343 \pm 0.0021$	$137.9325 \pm 0.0019$	137.9343 fixed
$T_{RVmax}$	$33\,018.15 \pm 0.23$	$33\,018.13 \pm 0.22$	$33\,018.43 \pm 0.25$	$33\,018.10 \pm 0.21$
$T_{Min,I}$	33 052.63	33 052.61	33 049.15	33 052.59
$T_{Min,II}$	32 983.66	32 983.64	32 986.98	32 983.62
$T_{periastr.}$	–	–	$33\,022.3 \pm 3.8$	–
$e$	0.0 fixed	0.0 fixed	$0.0520 \pm 0.0089$	0.0 fixed
$\omega$ (deg)	–	–	$11.1 \pm 9.9$	–
$K_1$ (km s $^{-1}$ )	$46.77 \pm 0.47$	$46.49 \pm 0.45$	$46.9 \pm 1.4$	$46.49 \pm 0.45$
$K_2$ (km s $^{-1}$ )	–	–	–	$29.6 \pm 1.7$
$\gamma_1$ (km s $^{-1}$ )	$7.95 \pm 0.76$	$7.90 \pm 0.75$	$8.17 \pm 0.63$	$7.90 \pm 0.75$
$\gamma_2$ (km s $^{-1}$ )	$6.4 \pm 1.1$	$6.4 \pm 1.2$	$6.6 \pm 1.0$	$6.4 \pm 1.1$
$\gamma_3$ (km s $^{-1}$ )	$9.6 \pm 1.1$	$9.6 \pm 1.2$	$8.9 \pm 1.1$	$9.7 \pm 1.2$
$\gamma_4$ (km s $^{-1}$ )	$6.9 \pm 1.2$	$6.8 \pm 1.2$	$6.7 \pm 1.2$	$6.8 \pm 1.2$
$\gamma_{14}$ (km s $^{-1}$ )	$9.2 \pm 3.2$	$9.2 \pm 3.2$	$10.1 \pm 3.6$	$9.2 \pm 3.2$
$\gamma_5$ (km s $^{-1}$ )	$14.63 \pm 0.78$	$14.69 \pm 0.77$	$14.47 \pm 0.77$	$14.68 \pm 0.77/14.3 \pm 1.1$
$\gamma_6$ (km s $^{-1}$ )	$11.6 \pm 2.1$	$11.7 \pm 2.1$	$12.2 \pm 2.6$	$11.7 \pm 2.1$
$\gamma_7$ (km s $^{-1}$ )	$14.12 \pm 0.60$	$14.18 \pm 0.58$	$14.10 \pm 0.58$	$14.17 \pm 0.58$
$\gamma_8$ (km s $^{-1}$ )	$6.83 \pm 0.91$	$6.83 \pm 0.90$	$6.5 \pm 1.0$	$6.79 \pm 0.86$
$\gamma_9$ (km s $^{-1}$ )	$10.2 \pm 1.4$	$10.1 \pm 1.4$	$9.9 \pm 1.2$	$10.1 \pm 1.4$
$\gamma_{10}$ (km s $^{-1}$ )	$9.94 \pm 0.90$	$9.82 \pm 0.88$	$10.07 \pm 0.85$	$9.82 \pm 0.89$
No. of RVs	211	211	211	211/11
rms (km s $^{-1}$ )	4.61	4.36	4.09	4.32/3.47

**Table 4.** Orbital solutions for two slightly overlapping subsets of older and more recent primary RVs to test the possibility of a secular change of the orbital period.

Time interval (HJD-2 400 000)	No. of RVs	$P$ (d)
13 743–34 975	104	$137.9449 \pm 0.0075$
29 500–53 674	124	$137.9257 \pm 0.0060$

variations on a time scale of some 20 days, i.e. similar to that of the observed light changes.

#### 4. The nature of the blue-shifted $H\alpha$ absorption

As already demonstrated by Bidelman (1949), Hack (1960), Nariai (1967, 1970), and Frame et al. (1995), a blue-shifted  $H\alpha$  absorption line was observed on some orbital cycles while missing in others. Published data on the presence and absence of the blue-shifted absorption in  $H\alpha$  were collected and schematically represented by Nariai (1967, 1970). Regrettably, there are only a few published  $H\alpha$  profiles from which one can measure central intensity  $I_c$  of the  $H\alpha$  absorption line. In particular, we measured  $I_c$  in the  $H\alpha$  profiles published by Hack (1960), Nariai (1967), and Frame et al. (1995).

All reliable observations suggest that in the cycles when the blue-shifted absorption line is observed, it attains the maximum strength around the conjunction with star 2 in front and virtually disappears at the other conjunction. Note in particular that Frame et al. (1995) obtained electronic  $H\alpha$  spectra of  $\nu$  Sgr covering parts of 12 consecutive orbital cycles in 1988, 1991, and 1992. Absolutely no trace of the blue-shifted  $H\alpha$  absorption is seen on these high-S/N spectra (see their Fig. 8) with the only exception of a single 1991 spectrogram (phase 0<sup>p</sup>.345 according to ephemeris (1)), which shows a strong  $H\alpha$  absorption with an RV of  $-360$  km s $^{-1}$  and a central intensity of 0.22. Instead,

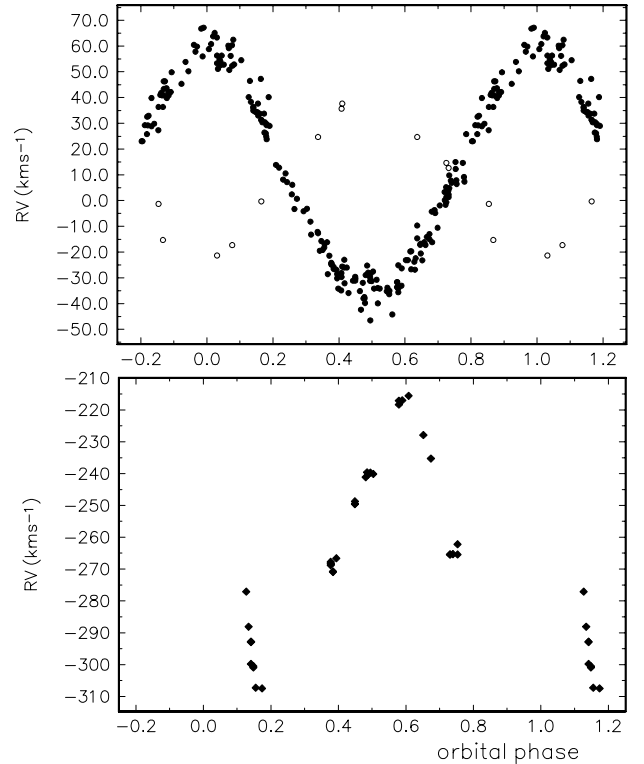


**Fig. 1.** Upper panel: RV curves of both binary components for solution 4. Bottom panel: the RV curve of the blue-shifted  $H\alpha$  absorption core. The RVs of the primary and secondary are shown by filled and empty circles, respectively, and those of the  $H\alpha$  absorption by diamonds.

their  $H\alpha$  profiles show the  $H\alpha$  emission with a steep blue edge and a very extended red wing reaching to some  $+500$  km s $^{-1}$ . The same type of  $H\alpha$  emission line with an extended red wing

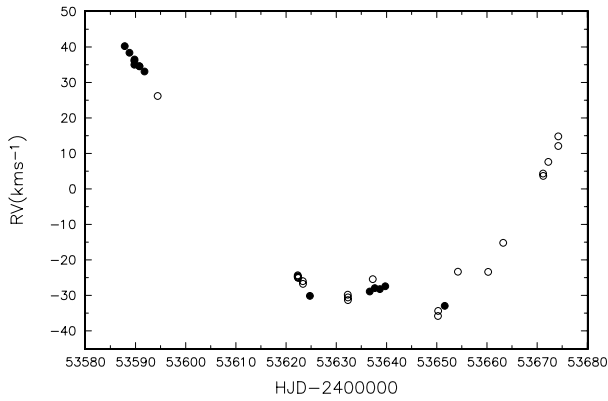


**Fig. 2.** DAO RVs (filled circles) and Ondřejov RVs (empty circles) of star 1 plotted vs. time. Small systematic deviations from a smooth orbital RV curve are seen and data from two independent spectrographs prove their reality.

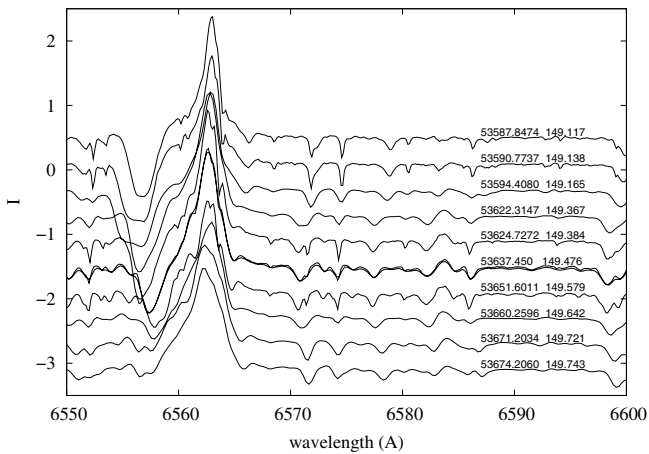


**Fig. 3.** Selected  $H\alpha$  line profiles from the DAO spectrograms showing the presence of a blue-shifted absorption of variable strength throughout the whole orbital cycle. Note that at phases when the line gets very weak, it is also blended with a telluric line at 6557 Å. The plot is constructed so as to permit a direct comparison with Fig. 8 of Frame et al. (1995). Note that the DAO spectra have a better spectral resolution than the Ondřejov spectra. For comparison, we also show 1 Ondřejov spectrogram taken at HJD 2 453 637.241. One can see that it nicely matches a DAO spectrogram taken shortly thereafter at HJD 2 453 637.659, which indicates that the line intensities from both data sets can be combined safely. (Note that a mean HJD is given for these two spectra in the plot.)

has already been observed by Greenstein (1943) in July and September 1940.

In contrast, *all*  $H\alpha$  line profiles obtained at DAO and Ondřejov between August and October 2005 *do show* the blue-shifted  $H\alpha$  absorption of variable intensity; see a representative selection of the  $H\alpha$  profiles in Fig. 3. The radial velocity of blue-shifted  $H\alpha$  absorption was also derived by comparing direct and reverse images of the line profile. Our measurements refer to the line core. The values of RVs from the phases when the satellite profiles are very faint are of course less reliable. On the other hand, the RV curve we obtained is smooth, changing continuously from phases where the satellite component dominates to phases where it gets faint. This could hardly be so if blending with some photospheric line takes place. In the interval of phases in question (around 0.8), the photospheric lines move in antiphase to the RV curve of the blue-shifted  $H\alpha$  absorption line.

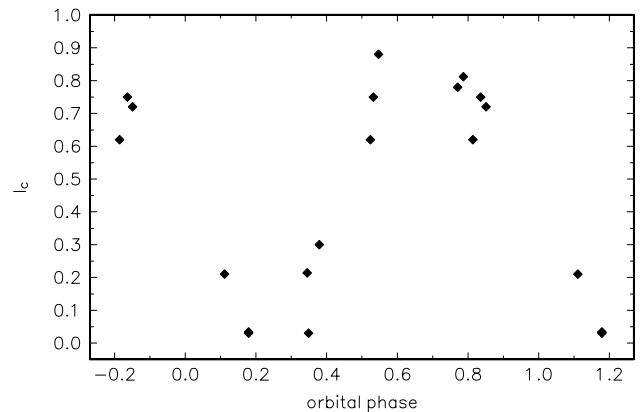
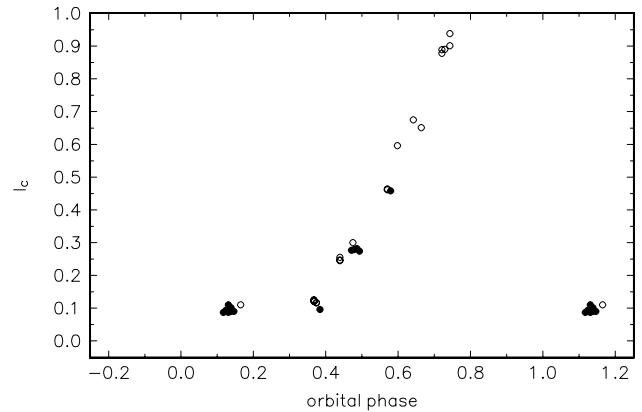


**Fig. 4.** Central intensities of the blue-shifted  $H\alpha$  absorption vs. phase of ephemeris (1): *upper panel*: our new DAO (filled circles) and Ondřejov (empty circles) electronic spectra; *bottom panel*: our measurements in the published  $H\alpha$  line profiles from Hack (1960), Nariai (1967), and Frame et al. (1995). One can see that the line indeed attains a maximum strength (i.e. minimal  $I_c$ ) at the conjunction with star 2 in front and a minimum at the other conjunction.

The RV curve of the blue-shifted  $H\alpha$  absorption is shown in the bottom panel of Fig. 1. From it we conclude that the RV behaviour of the  $H\alpha$  absorption does not support the Nariai (1967) interpretation in terms of a supersonic flow from the corona of star 1 extending to the vicinity of star 2. Very regrettably, our observations *do not cover* phase  $0^{\text{p}}25$  of the superior conjunction of star 1 where one would expect the largest negative RVs for his model. However, if the absorption were to originate from a stream flowing between the two stars, there would be no absorption seen in the elongation with star 1 approaching. Even if there were some self-absorption in the flow, its RV at these phases would be *close to the systemic velocity, which is certainly not the case*. We do confirm, however, the Nariai (1967) finding that the line attains its maximum strength at the superior conjunction of star 1 and minimum strength at the opposite one, when star 1 is in front – see Fig. 4. Note also a remarkable phase coherence in the line-strength variations for the earlier observed and new data. In other words, if the blue-shifted absorption is present in the spectra, its strength at any given orbital phase remains the same over many orbital cycles. This seems to indicate that the alternation between the presence and absence of this feature is probably a geometric, not physical effect.

Several authors have claimed that the blue-shifted absorption lines are also present in other Balmer lines and in some helium lines. In Fig. 5 we show a montage of the Ondřejov profiles of  $H\alpha$ ,  $H\beta$ ,  $H\gamma$ , and He I 6678. It is seen that, in the phases when

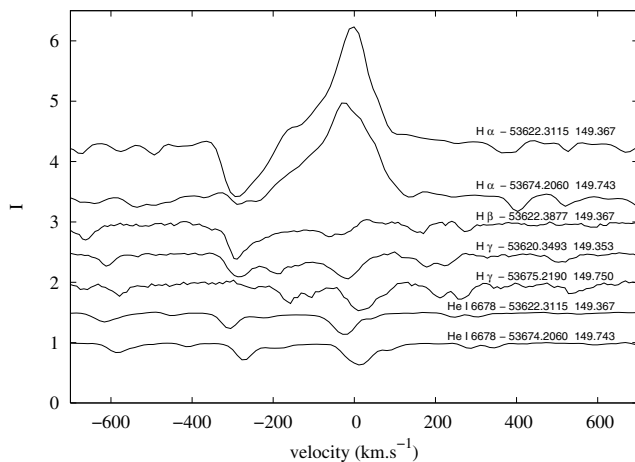


**Fig. 5.** Blue-shifted absorption lines of several Balmer lines from the Ondřejov CCD spectrograms. The same blue shift is observed for all three Balmer lines from similar orbital phases. Note also a good coherence of the phase variations of H $\alpha$  and H $\gamma$ ; HJD, cycle numbers, and phases are indicated as in Fig. 3. A line that looks like a blue satellite to He I 6678 moves in phase with it and represents therefore another spectral line of star 1.

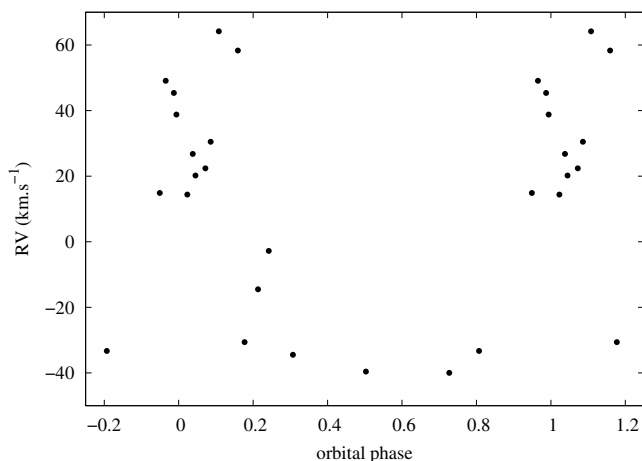


**Fig. 6.** The RV curve of a blue-shifted H $\beta$  absorption from Plaskett (1926). The original values were brought on the absolute velocity scale and shifted by  $272 \text{ km s}^{-1}$  to make the curve directly comparable to that shown in Fig. 1.

the blue-shifted H $\alpha$  absorption is strong, it is also observable in H $\beta$  and H $\gamma$ . There is no evidence, however, for a blue-shifted satellite line in He I 6678.

Plaskett (1926) published RVs of several putative blue-shifted absorption components of H $\beta$ , H $\gamma$ , H $\delta$ , and even He measured throughout the whole orbital cycle. In Fig. 6 we show the RV of one H $\beta$  satellite line transformed to the RV scale of Fig. 1. The resulting RV curve is reminiscent of the RV curve of star 1. This corroborates the conclusion by Greenstein (1950) that Plaskett (1926) probably misidentified some fainter lines of star 1 for the blue-shifted components of the Balmer lines.

## 5. The H $\alpha$ emission line

To have some idea about the location of the H $\alpha$  emission within the binary system, we measured the RV of the H $\alpha$  emission peak. Its variations with orbital phase are shown in Fig. 7. There is some disturbance near the conjunction with star 1 in front of

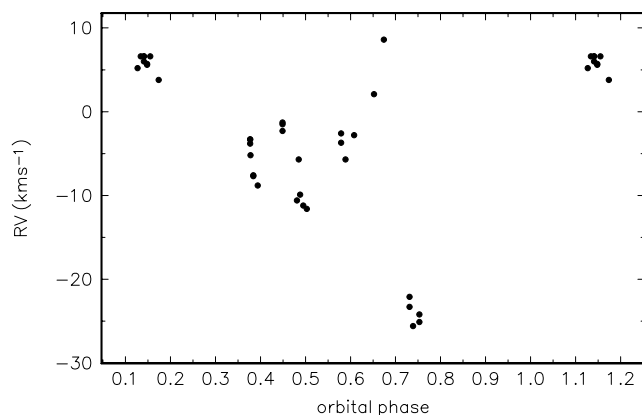


**Fig. 7.** Orbital RV curve of the H $\alpha$  emission peak.

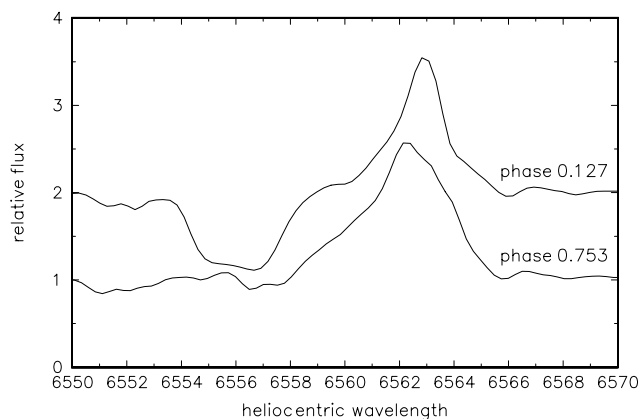


**Fig. 8.** A comparison of two Ondřejov H $\alpha$  line profiles taken shortly after one elongation and near the conjunction with star 1 in front.

star 2, leading to negative values of RV. Figure 8 compares two Ondřejov spectrograms obtained in orbital phases  $0^{\text{P}}127$  and  $0^{\text{P}}753$ . One can see that near the conjunction the emission line gets much wider, and there is probably some additional source of emission. Outside the conjunction phase, however, the emission RV seems to follow a sinusoidal variation almost in phase with star 1 but with a reduced amplitude. A formal orbital solution with the data near phase  $0^{\text{P}}75$  omitted leads to  $K = 10.1 \pm 5.2 \text{ km s}^{-1}$ ,  $\gamma = 3.4 \pm 0.8 \text{ km s}^{-1}$ ,  $T_{\text{RV max}} = \text{HJD } 2433009 \pm 2$ , the rms per 1 observation being only  $2.9 \text{ km s}^{-1}$ . A similar result was also found for the Fe II 6432 Å emission line, except that its RV curve is not disturbed near phase  $0^{\text{P}}75$ . This seems to indicate that the bulk of the emission originates in some area located on the same side from the binary centre of gravity as star 1.

## 6. Photometric variations

With the new accurate ephemeris, we compiled several representative  $V$  magnitude photometric data sets from the astronomical literature and plotted them vs. phase in Fig. 9. In particular we used the photometry of Eggen et al. (1950), Burnashev (1981), Manfroid et al. (1991), Sterken et al. (1993), Malcolm & Bell (1986), Frame et al. (1995), and Hipparcos  $H_p$  photometry (Perryman & ESA 1997) converted to the Johnson  $V$  magnitude following Harmanec (1998). One immediately sees that there is *no evidence* of photometric eclipses or ellipsoidal variations, although the observations of the lowest brightness of the object seem to cluster near phases  $0^{\text{P}}2-0^{\text{P}}3$  and  $0^{\text{P}}7-0^{\text{P}}8$ , which may

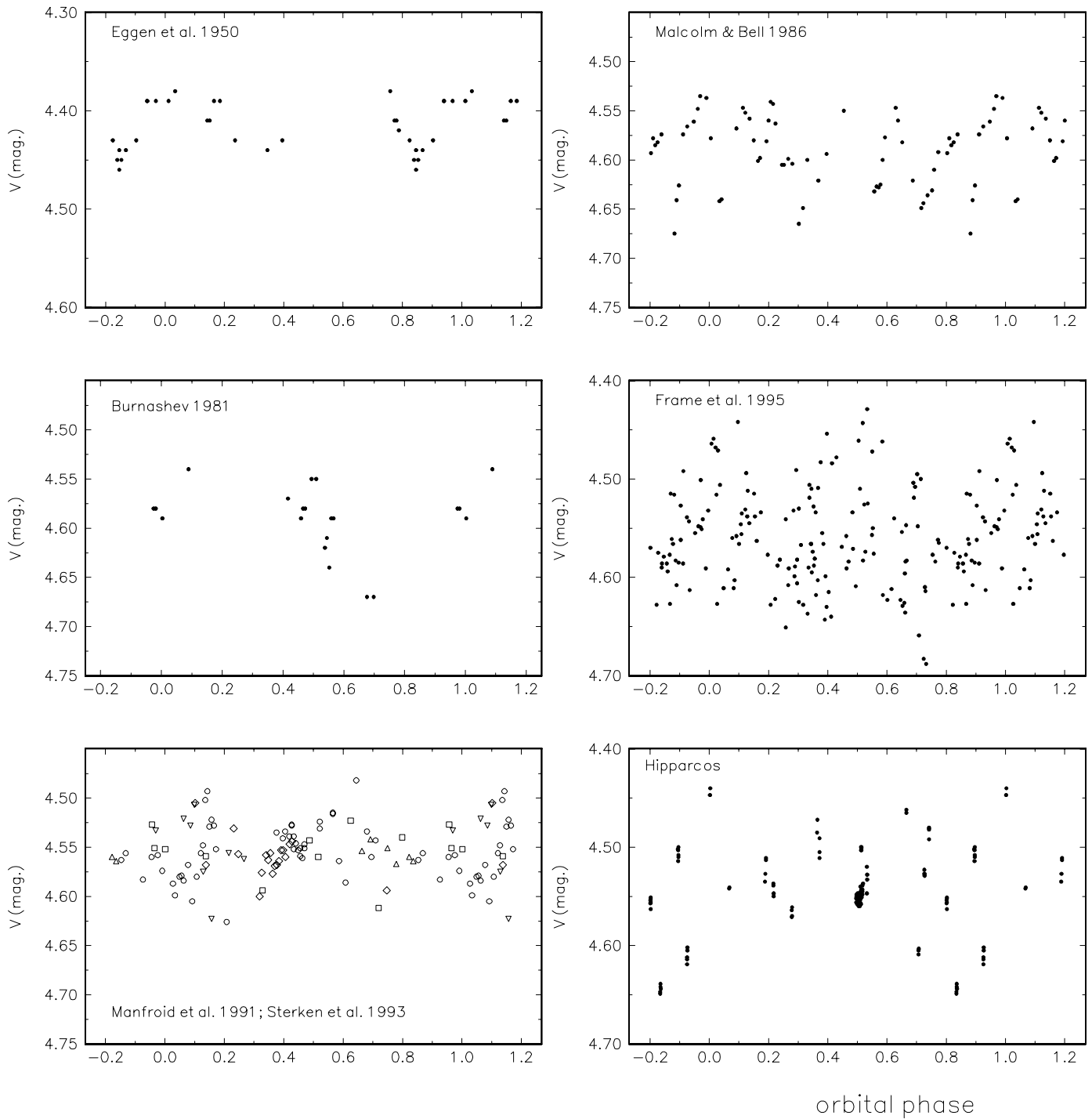


**Fig. 9.** Several orbital light curves for the  $V$ -magnitude observations found in the astronomical literature.

explain the early reports of eclipses. Figure 9 also illustrates the conclusion of Frame et al. (1995) that the amplitude of variations varies secularly with time. This implies that one remains empty-handed as far as the knowledge of the orbital inclination, and therefore binary masses, is concerned.

Analyzing the individual data sets for periodicity, we found that a time scale of 35–40 days is usually detected, leading to a double-wave light curve with two minima of different widths. Note that Malcolm & Bell (1986) found a twice shorter periodicity for a single-wave curve so that their findings probably refer to the same time scale of variations as ours. For illustration,

we show a phase plot of their  $V$  photometry for the best period of 40<sup>d</sup>.9611 in Fig. 10.

We intend to re-observe all comparison stars used by different observers to be able to homogenize the existing data sets and combine them for a future period analysis.

## 7. Towards understanding the properties and nature of $\nu$ Sgr

After a critical re-examination of the observational evidence, we conclude that one should remain open-minded when interpreting

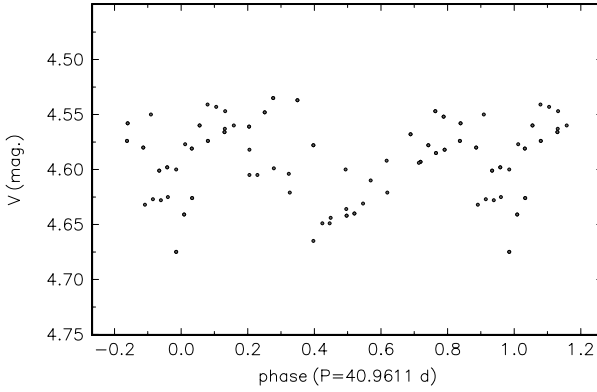


**Fig. 10.** A phase plot of Malcolm & Bell (1986)  $V$  photometry for the best “period” of 40.9611. Two minima of different width in one cycle are seen.

the geometry and evolutionary stage of  $\nu$  Sgr. We also suggest a few hints.

1. The fact that there is no evidence of eclipses leaves room to also consider models that include structures like an optically thick accretion disk and bipolar jets perpendicular to the orbital plane. Such structures are known for another well-known peculiar binary  $\beta$  Lyr – see Harmanec (2002) and references therein. If the emission and the blue-shifted (self-)absorption of  $H\alpha$  observed for  $\nu$  Sgr also originates in such jets (with large expansion velocities), then a precession of the binary orbit, or at least of the disk and associated jets, would probably provide a way of explaining why the blue-shifted  $H\alpha$  absorption is only seen at certain intervals of time and missing in others, while the  $H\alpha$  emission moves in phase with star 1 but with a reduced amplitude. Again, the existence of such putative structures could be confirmed or disproved via interferometry even if the orbit itself would not be resolved.
2. We also suggest that the peculiar spectrum of star 1 that combines lines of low and high degrees of ionization may actually be the spectrum of *the disk rim and disk face*. In contrast to  $\beta$  Lyr seen almost edge-on where one only observes the disk rim, the lower orbital inclination of  $\nu$  Sgr would permit us to also see the disk face, illuminated by the hotter central object. It is true that Greenstein & Adams (1947) had already argued that the line spectrum of star 1 is not consistent with the nebular densities expected for the disk and that this wide range of densities may be a result of the lower opacity related to the hydrogen deficiency in the atmosphere. This, however, does not contradict our alternative interpretation that the line spectrum is a kind of pseudo-photosphere of an optically thick disk, similar to the one seen in  $\beta$  Lyr.
3. Note also that if our finding that the bulk of material producing emission lines moves with reduced amplitude almost *in phase* with star 1 is confirmed by more numerous RV measurements in the future, it might provide additional support to the idea of bipolar jets associated with the disk of star 1.
4. An obvious problem of this interpretation is that one would need to postulate that the mass-gaining object is star 1, not star 2 as believed so far. This is weakly supported by the  $1-\sigma$  result that the orbital period is decreasing, but one then has the problem of why the more massive and now supposedly mass-losing star 2 is not seen in the optical spectra. If star 2 were filling its Roche lobe, larger than that of star 1, it would be the brighter of the two. One could

**Table 5.** Probable basic physical properties of  $\nu$  Sgr based on orbital solution 4 of Table 3 derived for three possible values of the orbital inclination. Tabulated are masses  $M_1$  and  $M_2$ , the semi-major axis  $A$ , Roche-lobe radii  $R_1^{\text{Roch}}$  and  $R_2^{\text{Roch}}$ , and the minimum and maximum angular dimensions of the semi-major axis  $a_{\text{min}}$  and  $a_{\text{max}}$ , derived for the range given by the Hipparcos parallax and its error  $p = 0''.00195 \pm 0''.00072$ .

Element	$i = 70^\circ$	$i = 50^\circ$	$i = 30^\circ$
$M_1 (M_\odot)$	2.95	5.45	19.6
$M_2 (M_\odot)$	4.64	8.56	30.8
$A (R_\odot)$	220.7	270.8	414.8
$R_1^{\text{Roch}} (R_\odot)$	73.7	90.3	138.4
$R_2^{\text{Roch}} (R_\odot)$	92.0	112.8	172.9
$a_{\text{min}} (")$	0.0013	0.0015	0.0024
$a_{\text{max}} (")$	0.0027	0.0034	0.0052

consider mass loss and mass transfer due to the rotational instability of star 2 near its rotational  $L_1$  point, such as studied by Harmanec et al. (2002). In that case, star 2 could have a much smaller radius and be less luminous than the disk around its counterpart, but such a model is purely speculative at the moment.

Based on solution 4 of Table 3, one obtains the mass function  $f(M) = 1.436 M_\odot$  and a mass ratio  $M_2/M_1 = 1.57$ . Since it is obvious that there are no longer any strong arguments to assume that we observe the binary nearly equator-on, we estimate the probable basic physical properties of  $\nu$  Sgr for three possible orbital inclinations – see Table 5. Given the absence of deep binary eclipses, inclinations higher than about  $70^\circ$  are improbable. We also tabulate the angular dimension of the projected semi-major axis in the sky, using the Hipparcos parallax  $p = 0''.00195 \pm 0''.00072$  (Perryman & ESA 1997). We recall, however, that the secondary RV curve needs verification and that the actual mass ratio and, therefore, the system dimensions could be quite different.

Nevertheless, it seems that the most powerful of the already operating optical interferometers might be potentially able to resolve this binary, an attempt that is worth the effort. At the same time it is clear that the interferometry of  $\nu$  Sgr could substantially help to restrict the possible classes of models for this peculiar binary. The most important would be an interferometric determination of the orbital inclination of  $\nu$  Sgr which – together with an independent confirmation of the RV curve of star 2 – would finally settle the question of the true masses of both bodies.

*Acknowledgements.* We acknowledge the use of the programs SPEFO and FOTEL, made available by their authors Drs. Jiří Horn and Petr Hadrava. Our thanks are also due to Dr. Peter Cottrell, who kindly clarified the problem with Mt. John’s RVs for us. Very relevant comments, suggestions, and a constructive criticism by the anonymous referee helped to improve the paper and are gratefully acknowledged. We profited from the use of the electronic bibliography maintained by the NASA/ADS system. Czech authors were supported by the research plan AV OZ1 003909, from project K2043105 of the Academy of Sciences of the Czech Republic, and from the grants GA ČR 205/02/0788 and 205/06/0584. The research of PH was also supported from the grant GA ČR 205/06/0304 of the Czech Science Foundation.

## References

- Bidelman, W. P. 1949, ApJ, 109, 544  
 Burnashev, V. I. 1981, Izvestiya Krymskoj Astrofizicheskoj Observatorii, 63, 104  
 Campbell, W. W. 1895, ApJ, 2, 177  
 Campbell, W. W. 1899, ApJ, 10, 241  
 Dudley, R. E., & Jeffery, C. S. 1990, MNRAS, 247, 400  
 Dudley, R. E., & Jeffery, C. S. 1993, MNRAS, 262, 945



- Duvignau, H., Friedjung, M., & Hack, M. 1979, *A&A*, 71, 310
- Eggen, O. J., Kron, G. E., & Greenstein, J. L. 1950, *PASP*, 62, 171
- Eggleton, P. P. 2002, *ApJ*, 575, 1037
- Frame, D. J., Cottrell, P. L., Gilmore, A. C., Kilmartin, P. M., & Lawson, W. A. 1995, *MNRAS*, 276, 383
- Frost, E. B., Barrett, S. B., & Struve, O. 1926, *ApJ*, 64, 1
- Gaposchkin, S. 1945, *AJ*, 51, 109
- Greenstein, J. L. 1943, *ApJ*, 97, 252
- Greenstein, J. L. 1950, *ApJ*, 111, 20
- Greenstein, J. L., & Adams, W. S. 1947, *ApJ*, 106, 339
- Greenstein, J. L., & Merrill, P. W. 1946, *ApJ*, 104, 177
- Hack, M. 1960, *Contr. Oss. Astr. Milano-Merate*, 152, 1
- Hack, M. 1980, in *Close Binary Stars: Observations and Interpretation*, IAU Symp., 88, 271
- Hack, M., & Pasinetti, L. 1963, *Contr. Oss. Astr. Milano-Merate*, 215, 1
- Hadrava, P. 2004, *Publ. Astron. Inst. Acad. Sci. Czech Rep.*, 92, 1
- Harmanec, P. 1985, *Bull. Astron. Inst. Czechoslovakia*, 36, 327
- Harmanec, P. 1998, *A&A*, 335, 173
- Harmanec, P. 2002, *Astron. Nachr.*, 323, 87
- Harmanec, P., Bisikalo, D. V., Boyarchuk, A. A., & Kuznetsov, O. A. 2002, *A&A*, 396, 937
- Hill, G., Harmanec, P., Pavlovski, K., et al. 1997, *A&A*, 324, 965
- Horn, J., Kubát, J., Harmanec, P., et al. 1996, *A&A*, 309, 521
- Jaschek, M., Jaschek, C., & Andrillat, Y. 1990, *A&A*, 232, 126
- Jeffery, C. S., Drilling, J. S., & Heber, U. 1987, *MNRAS*, 226, 317
- Koubský, P., Harmanec, P., Kubát, J., et al. 1997, *A&A*, 328, 551
- Leushin, V. V. 2001, *Astron. Lett.*, 27, 634
- Malcolm, G. J., & Bell, S. A. 1986, *MNRAS*, 222, 543
- Manfroid, J., Sterken, C., Bruch, A., et al. 1991, *A&AS*, 87, 481
- Maury, A. C. 1925, *Harvard College Observatory Bulletin*, 824, 4
- Nariai, K. 1967, *PASJ*, 19, 564
- Nariai, K. 1970, *PASJ*, 22, 559
- Parthasarathy, M., Cornachin, M., & Hack, M. 1986, *A&A*, 166, 237
- Perryman, M. A. C., & ESA. 1997, *The HIPPARCOS and TYCHO catalogues*, Noordwijk, Netherlands: ESA SP-1200
- Plaskett, J. S. 1926, *Publ. Dominion Astrophys. Obs. Victoria*, 4, 1
- Plavec, M. J. 1986, in *Hydrogen Deficient Stars and Related Objects*, *ASSL*, 128, IAU Colloq., 87, 231
- Schoenberner, D., & Drilling, J. S. 1983, *ApJ*, 268, 225
- Škoda, P. 1996, in *Astronomical Data Analysis Software and Systems V*, *ASP Conf. Ser.*, 101, 187
- Sterken, C., Manfroid, J., Anton, K., et al. 1993, *A&AS*, 102, 79
- Treffers, R., Woolf, N. J., Fink, U., & Larson, H. P. 1976, *ApJ*, 207, 680
- Wilson, R. E. 1913, *Lick Observatory Bulletin*, 8, 132